

Numerical simulation of greening effects for idealised roofs with regional climate forcing

GÜNTER GROSS*

Institut für Meteorologie und Klimatologie, Universität Hannover, Germany

(Manuscript received January 31, 2011; in revised form February 15, 2012; accepted February 16, 2012)

Abstract

A numerical model was used to simulate temperature distribution in and above an extensive green roof with a long term forcing adopted from a regional climate model. Time variations of temperature for different time scales ranging from days to decades have been calculated. The results are in good agreement with selected field experiments and generally reinforce the understanding prevailing in literature regarding temperature differences of green roofs compared to a concrete roof. Green roofs result in a significant reduction of daytime human heat load and an improvement of thermal comfort conditions, while during night-time a concrete roof favours low temperatures and a low number of minimum temperatures above 20 °C (tropical nights). A future shift in seasonal precipitation would necessitate irrigation in the summer months to ensure the vitality of roof vegetation. An estimation of the amount of additional watering and the increased number of watering days per year is given.

1 Introduction

Global and regional climate scenarios suggest an increase of annual mean near surface temperature in Central Europe by 3–4 K by the end of this century. Together with an expected change in the seasonality of precipitation with wetter winters and drier summers our environment will be very different compared to the present situation (IPCC, 2007).

This climate change will also impact the urban environment where people nowadays are still confronted with significantly higher temperatures than in the surrounding rural areas. Besides an additional warming, which increases the risk of biophysical loads as summarized e.g. by JENDRITZKY et al. (2009) or MUTERS et al. (2010), for German cities also changes in urban hydrology with more heavy precipitation events as well as longer drought periods in summer are expected. More summer days with calm winds and undisturbed solar radiation will cause additional ozone and air pollution problems (KUTTLER, 2011). One facet of adapting cities and inhabitants to a climate change is an effective use of green infrastructures like parks and green walls and roofs in the urban area (WILBY, 2007, GILL et al., 2007). Evapotranspiration from vegetation results in a greater fraction of solar radiation contributing to latent heat fluxes, damping local near-surface temperature extremes. This process helps to keep buildings cool in summer and reduces their energy consumption (TEEMUSK and MANDER, 2009).

In many field experiments the cooling effect of a green cover of roofs or building walls has been demon-

strated (e.g. TAKEBAYASHI and MORIYAMA, 2007; LIU and BASKARAN, 2003; HARAZONO et al., 1990). However, an extrapolation to a larger urban area or the estimation of a combined effect of a larger number of different green spaces on urban climate is difficult.

Complementary tools include numerical models which are applicable to describe heat transfer in roof and façade material of complex structures as well as the wall-air interaction near the surface. Models of different complexity are available and have been used for a wide variety of problems in the field of green cover and urban climate (TAKAKURA et al., 2000; ALEXANDRI and JONES, 2007, 2008; HUTTNER et al., 2008).

Limited knowledge exists about the results for a model system linking regional climate change with a micro scale model for specific roof structures. A first step in this direction will be presented in this paper.

In this paper a one-dimensional single column time-dependent surface layer model is introduced which can be used to simulate temperature distribution above and inside an idealised roof of different structures and components. The roof in this study is an infinite surface. Effects of edges and corners on wind and turbulence are not considered here. Forced by the results of a regional climate model, long term time series are simulated in order to evaluate mean temperature in and above a roof as well as for selected biometeorological measures.

2 The model

The numerical model system introduced here must be able to simulate the interactions between the near surface atmosphere and the underlying inner structured green roof for a given long-term external forcing. Therefore, an energy balance model was combined with a

*Corresponding author: Günter Gross, Institut für Meteorologie und Klimatologie, Universität Hannover, Herrenhäuser Str. 2, 30419 Hannover, e-mail: gross@muk.uni-hannover.de

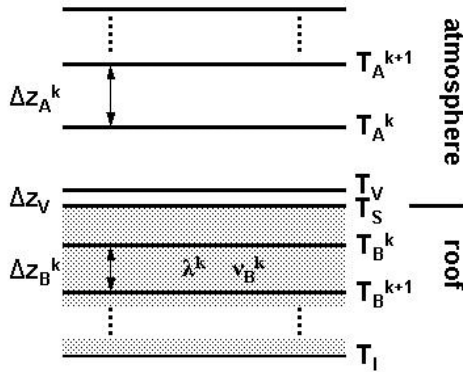


Figure 1: Schematic view of layer distribution and notation. Thick lines are calculation levels numbered with index k in the atmosphere and inside the roof.

simple one-dimensional (with respect to the vertical) surface layer model, while the external forcing was adopted from a regional climate model. Due to the one-dimensional assumption, the model simulation represents a horizontally homogeneous, extensive uniform roof neglecting border effects.

2.1 Surface heat budget

The temperature at the roof surface is determined by a surface energy budget, which includes sensible and latent heat flux (Q_H) and (Q_V), heat transfer in the underlying structured roof or soil material (Q_B) as well as long-wave (Q_L) and short-wave radiation (Q_S). An anthropogenic heat release is not considered here. To derive the heat budget at the surface (index s), the structure given in Figure 1 was adopted.

Equations and notations are conventional (e.g. STULL, 1988) and the surface heat budget reads

$$Q_S + Q_V + Q_H + Q_L + Q_B = 0 \quad (2.1)$$

Positive sign is used for energy gain of the surface, negative sign for energy loss. Short-wave radiation is calculated by

$$Q_S = (1 - a)I_0 \sin(h) \quad (2.2)$$

with albedo (a), solar irradiance (I_0) and zenith angle (h), depending on location and time (e.g. GROSS, 1993).

For the net outgoing long-wave radiation the outgoing part according to Stefan Boltzmann law

$$Q_L = -\varepsilon\sigma T_S^4 \quad (2.3)$$

with surface emissivity (ε) as well as the downward directed long-wave radiation flux have to be considered. The downward directed part from the atmosphere is adopted from the results of the regional climate model without modifications. Flux-gradient relationships have been used to determine latent and sensible heat flux

$$Q_H = c_p \rho K \frac{\partial T}{\partial z} = c_p \rho K \frac{T_A^1 - T_S}{\Delta z_A^1} \quad (2.4)$$

$$Q_V = L_s \rho K \frac{\partial s}{\partial z} = L_s \rho K \frac{s_A^1 - s_S}{\Delta z_A^1} \quad (2.5)$$

s is specific humidity, K turbulent exchange coefficient, c_p and L_s specific and latent heat and ρ air density. The index S means surface and A the first grid level in the atmosphere.

The heat flux into the underlying material Q_B is calculated for different locations inside the roof (Δz is the thickness of the first inner layer, see Figure 1) with thermal conductivity λ by

$$Q_B = -\lambda \frac{\partial T}{\partial z} = -\lambda \frac{T_S - T_B^1}{\Delta z_B^1} \quad (2.6)$$

while for the temperature inside the material, T_B , the heat conduction equation

$$\frac{\partial T_B}{\partial t} = \nu_B \frac{\partial^2 T_B}{\partial z_B^2} \quad (2.7)$$

with thermal diffusivity ν_B is used. Depending on the inner structure of the roof, very different values for ν_B are specified for each layer.

For smooth surfaces (e.g. concrete, bituminous concrete) very large temperature gradients close to the ground can be observed. However, the assumption of an effective turbulent sensible heat flux also directly at the ground would prevent such extreme gradients. For this reason, an additional thin micro layer where molecular processes dominate, was included as the interface between the smooth roof surface and the atmosphere. With the assumption that the molecular heat flux at the surface is equal to the turbulent heat flux at the top of the micro layer (STULL, 1988), a temperature T_V at the top of the viscous layer can be calculated as

$$T_V = \frac{T_S + c_1 T_A^1}{1 + c_1} \quad (2.8)$$

with

$$c_1 = \frac{K \Delta z_V}{\nu_L \Delta z_A^1}$$

with $\nu_L = 1.5 \cdot 10^{-5} \text{ m}^2 \text{ s}^{-1}$ for air and a viscous layer depth $\Delta z_V = 0.5 \text{ mm}$.

2.2 The simple surface layer model

The knowledge of different meteorological variables near the surface is essential for the calculation of various components of the heat budget equation. The forcing of the model will be the output of a regional climate model for a height of 10 m above ground. Therefore only the variations of wind, temperature and humidity in the lowest 10 m have to be calculated by the simple meteorological model. For wind speed (u), potential temperature (θ) and specific humidity (s) a diffusion equation is adopted, while the turbulent diffusion coefficient has

been calculated using the Prandtl-Kolmogorov relation via the turbulent kinetic energy (E).

$$\frac{\partial \psi}{\partial t} = \frac{\partial}{\partial z} K \frac{\partial \psi}{\partial z}, \psi = [u, \theta, s] \quad (2.9)$$

$$\frac{\partial E}{\partial t} = \frac{\partial}{\partial z} K \frac{\partial E}{\partial z} + K \left(\frac{\partial u}{\partial z} \right)^2 - K \frac{g}{\theta} \frac{\partial \theta}{\partial z} - \frac{E^{3/2}}{l} \quad (2.10)$$

$$K = c_2 l \sqrt{E}, \quad c_2 = 0.2 \quad (2.11)$$

The effects of thermal stability on turbulent mixing in the lower boundary layer will roughly be considered by a stratification dependent mixing length

$$l = l_a / \phi \quad (2.12)$$

$$l_a = \kappa z, \quad \kappa = 0.41 \quad (2.13)$$

ϕ represents the local universal function which may according to BUSINGER et al. (1971) be expressed as

$$\phi = 1 + \gamma_1 \frac{z}{L} \quad \text{for} \quad \frac{\partial \theta}{\partial z} > 0 \quad (2.14)$$

$$\phi = (1 - \gamma_2 \frac{z}{L})^{-0.25} \quad \text{for} \quad \frac{\partial \theta}{\partial z} \leq 0 \quad (2.15)$$

with $\gamma_1 = 4.7$ and $\gamma_2 = 15$. L denotes the Monin-Obukhov stability length. More details are given by GROSS (1993).

In this study $\kappa = 0.41$ is used as published by DYER (1974) ($\kappa = 0.41$ together with $\gamma_1 = 5.0$ and $\gamma_2 = 16$) instead of $\kappa = 0.35$ as found by BUSINGER et al. (1971) for $\gamma_1 = 4.7$ and $\gamma_2 = 15$. This inconsistent parameter combination used here results in small differences for e.g. wind and temperature at specific times. The general findings published in this study are not affected by this inconsistency.

2.3 Boundary conditions and numerical aspects

The lower boundary conditions are zero wind speed, turbulent kinetic energy proportional to friction velocity squared and surface temperature according to the result of the surface heat budget. For smooth surfaces T_V according to equation (2.8) is used instead of T_S . Friction velocity is calculated assuming a log+linear wind profile from the lower boundary up to the first grid level in the atmosphere. For specific humidity a completely dry surface is assumed for the concrete roof where all precipitation is removed by drainage systems completely and immediately. On the other hand a sufficient water supply

all the time is adopted whenever green is at the surface. In this case specific humidity is equal to the saturation specific humidity at the actual temperature.

The temperature at the interior boundary of the roof (T_I) is calculated by a simplified heat budget equation, where the energy fluxes from the roof and from the interior are considered:

$$0 = \lambda \frac{T_B - T_I}{\Delta z_B} + \alpha (T_{room} - T_I) \quad (2.16)$$

with heat transfer coefficient α ($\alpha = 25 \text{ W m}^{-2} \text{ K}^{-1}$) and interior temperature T_{room} ($T_{room} = 20 \text{ }^\circ\text{C}$).

At the upper boundary at 10 m height, the values for wind, temperature and humidity will be specified according to the results of the regional climate model CLM (ROCKEL et al., 2008). This model assumption implies that all disturbances generated at the roof surface have vanished at this height. However, for specific times of the integration period, especially for very unstable thermal conditions, the validity of this assumption is not always guaranteed.

The regional climate model CLM has been developed on the basis of the routinely used weather forecast model LM of the German Meteorological Service. It has been tested and validated for a wide variety of meteorological variables (e.g. HOLLWEG et al., 2008). Especially for climatological measures for the 10 m wind, modelled and observed data show only small deviations (WALTER et al., 2006).

The results of the CLM model runs are available for different future scenarios with a time resolution of 3 hours for the next 100 years. A description of the numerical experiments including input parameters, different realisations and forcing is given by HOLLWEG et al. (2008). In this study the results for the A1B_1_D3 scenario (LAUTENSCHLAGER et al., 2009) at the grid point located closest to Hannover will be used for wind speed, temperature, specific humidity and downward directed long-wave radiation flux. Within the 3 hour CLM time intervals a linear interpolation was used. In order to consider the reduction of direct solar radiation due to clouds or other aerosols, a factor was determined every 3 hours by the calculated CLM value and the theoretical expected astronomical value. This factor was constant for 3 hours and was used to calculate the short wave radiation at every small time step in the heat budget equation.

The prognostic equations are integrated forward in time for the period 2000–2100 with a time step of 600s on 12 grid levels in the atmosphere at heights of 0.25, 0.5, 0.75, 1, 1.5, 2, 2.5, 3, 4, 5, 6 and 8 m and in the soil in depths of 7, 14, 21 and 30 cm.

3 Results

3.1 Comparison with observation

In order to estimate the reliability of the model, a comparison with published experimental results has been

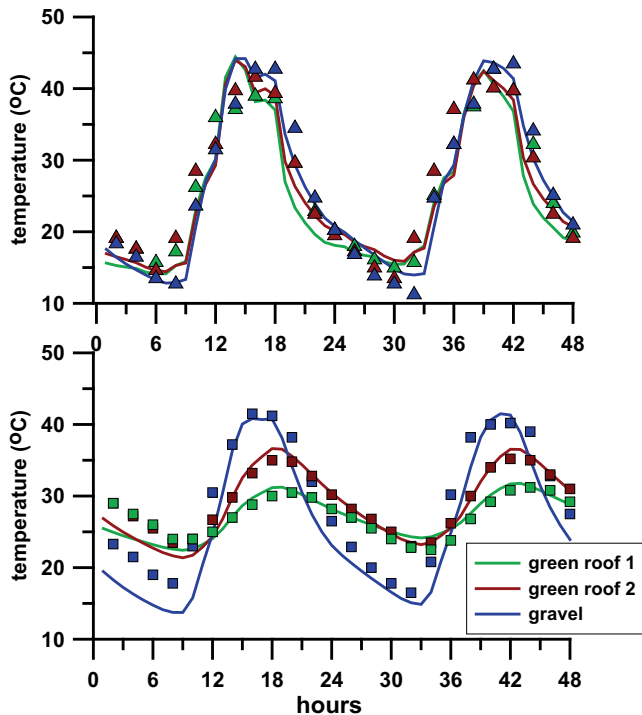


Figure 2: Diurnal variation of surface temperature (above) and temperature below the sub-strates (below). Solid lines are numerical results, symbols are observations (after KÖHLER and MALORNY, 2009).

performed. KÖHLER and MALORNY (2009) describe observations of long term experiments for different roof structures, which can be used for such a first estimate. Different meteorological parameters have been observed in and above green roofs as well as for a conventional gravel roof. The roof structure consists of 25 cm concrete and 14 cm insulation covered by a 10 cm growth media layer (green roof 1 = Optima, green roof 2 = Ulopor) with different thermal properties or covered by gravel. The soil grid levels have been adapted to this experimental design.

A two-day period from August 6 to August 7 in 2004 has been described in more detail and was used here for comparisons. Besides the material constants given in the paper (e.g. $\lambda = 0.37 \text{ Wm}^{-1}\text{K}^{-1}$ and $\lambda = 0.21 \text{ Wm}^{-1}\text{K}^{-1}$ for the green roofs, $\lambda = 2.1 \text{ Wm}^{-1}\text{K}^{-1}$ for gravel), additional weather information for the specific August days were adopted from the German Meteorological Service. The weather during this period was dominated by a high pressure system with mostly cloudless sky and an undisturbed insolation. Wind speed was around $2\text{--}4 \text{ ms}^{-1}$ and temperatures between 19°C at night and 25°C during the day. For the remaining parameters not described in the publication (e.g. albedo, emissivity), standard values after HUPFER and KUTTLER (2006) are used. Due to numerous uncertainties in the input parameters, one can not expect a perfect reproduction of the detailed observations by the model. How-

ever, the main characteristics of the temperature distribution with time should be covered by the model.

Due to undisturbed insolation, a well pronounced diurnal variation of temperature was observed with surface values well above 40°C (Figure 2). The underlying substrate was relatively dry during these days and, consequently, evapotranspiration plays only a minor role. Therefore, the surface temperature amplitudes for the different materials are quite similar. The simulated results follow the observations, whereby amplitudes as well as phase show a very reasonable agreement. Due to the different thermal properties of the substrates, heat penetrates with different amplitudes and phase shifts into the underlying structure. Observations at the bottom of the substrate layers show a significant amplitude damping for the green roofs compared to the gravel situation. The temperature decrease is up to 10 K during daytime and also a phase shift is evident. Due to the inaccurate knowledge of the initial conditions, simulated temperatures in the first night show larger differences to the observations. However, after sunrise the strong external forcing dominates the surface heat budget and amplitudes as well as phase follow the observations very reasonably.

The comparison given above demonstrates the applicability of the model system in principle. The agreement between simulation and observations was not perfect but satisfactory. A part of the differences must be attributed to the limited knowledge of subsoil properties for a living surface with varying water availability.

3.2 Numerical experiments

Numerical simulations with the model system have been performed for 100 years for different experimental roofs. The reference roof consists of pure concrete with a thickness of 30 cm covered alternatively also with a thin bituminous layer. The green roof is placed upon such a concrete roof with an additional thermal insulation layer of 10 cm and a soil layer of 10 cm with short, evergreen vegetation. A schematic view of the roof structure with the assignment of soil and roof parameter is given in Figure 3, the numerical values (HUPFER and KUTTLER, 2006; GAFFIN et al., 2009) in Table 1.

Results will be compared with respect to very different time scales ranging from days to decades and larger in order to estimate the characteristic effects of a green roof for a wide variety of weather conditions.

In Figure 4 the diurnal variation of different meteorological variables is shown. This period of a week is characterized by clear sky conditions with nearly undisturbed incoming shortwave radiation. Consequently the surface temperature for all roof structures follows this forcing with well pronounced diurnal cycles. The bituminous roof with a low albedo shows the largest heating with maximum temperatures around 70°C around noon. A larger albedo value lowers this maximum by almost 10 degrees. During night-time the emission of longwave

Table 1: Surface, soil and roof parameter used for the numerical experiments.

roof	albedo	emissivity	thermal conductivity [λ] = $\text{Wm}^{-1}\text{K}^{-1}$	thermal diffusivity [ν] = m^2s^{-1}	roughness length [z_o] = m
concrete	$a_1=0.25$	$\varepsilon_1=0.96$	$\lambda_1=1.5$	$\nu_1=0.7 \cdot 10^{-6}$	$z_o=0.01$
Bituminous concrete	$a_2=0.05$	$\varepsilon_2=0.96$	$\lambda_1=1.5$	$\nu_1=0.7 \cdot 10^{-6}$	$z_o=0.01$
green	$a_3=0.19$	$\varepsilon_3=0.97$	$\lambda_3=2.2$	$\nu_{31}=0.7 \cdot 10^{-6}$ $\nu_{32}=0.1 \cdot 10^{-6}$ $\nu_1=0.7 \cdot 10^{-6}$	$z_o=0.03$

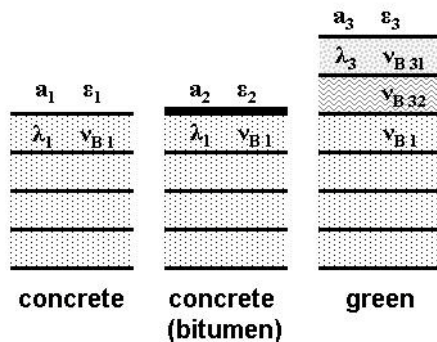


Figure 3: Roof structures and notation.

radiation cools the smooth surface significantly resulting in a temperature variation between day and night of 50–60 degrees. In contrast, the green roof uses the incoming solar radiation during daytime also for evapotranspiration resulting in an evident reduction of maximum temperature. During night time minimum temperatures of the surfaces are very similar for all roof structures with slightly higher values for the green roof.

The surplus of energy will be transferred into the atmosphere as well as into the underlying roof. Inside the roof, molecular conduction is the primary transport process resulting in periodic temperature variation that decreases in amplitude and increases in phase lag with increasing depth. The amount of change inside the roof depends on local subsoil parameters. A large thermal diffusivity like in concrete coincides with an efficient heat transfer and a significant diurnal temperature variation also at the inner side of the roof. The insulation of the green roof is responsible for a very uniform diurnal temperature of T_I (LIU and MINOR, 2005). Such typical diurnal variations of roof temperatures have also been observed in different field experiments (e.g. TAKAKURA et al., 2000; HARAZONO et al., 1990).

Surface temperature increases significantly at day 4 of the selected period, although solar radiation remains nearly unchanged. The reason is a reduction of wind speed which lowers the effect of turbulent and latent heat fluxes and the remaining energy fluxes in the heat budget are in balance at a higher surface temperature.

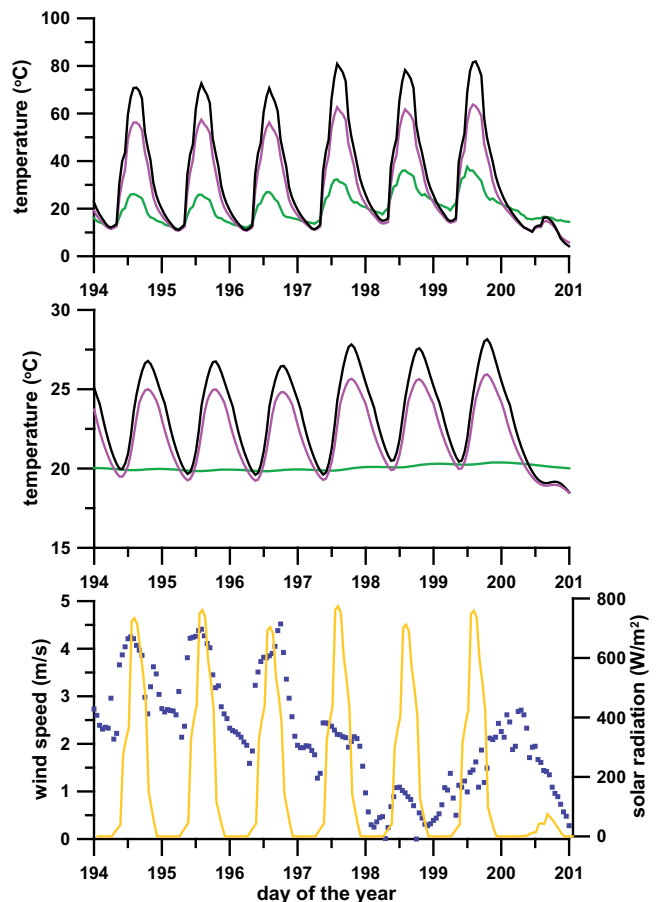


Figure 4: Diurnal variation of surface temperature (top), temperature at the lower side of the roof T_I (middle) for different insolation (yellow) and wind (blue) conditions (below). Magenta: Concrete roof, black: bituminous concrete, green: green roof.

In Figure 5 a time height cross-section for temperature for two days of the one week period from above is given. Note the different scales with meters in the atmosphere and decimeters in the roof. The surface of the concrete roof is heated around noon and energy is distributed into the atmosphere as well as into the material of the underlying structure. Due to the uniform thermal diffusivity temperature penetrates effectively into the roof with a decrease in amplitude and an increase in phase lag. The warming of the green roof’s surface is much lower due to evapotranspiration effects, while

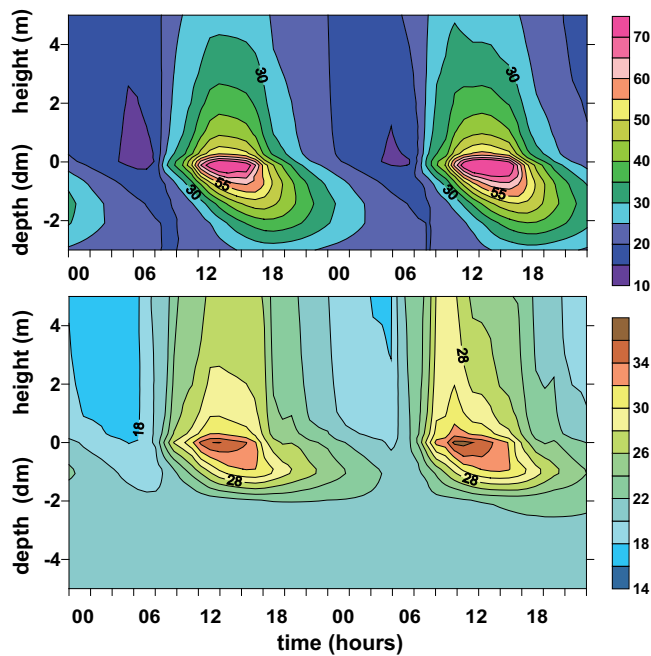


Figure 5: Time-height cross section of temperature (in °C) in the roof and in the atmosphere for the concrete roof (above) and the green roof (below).

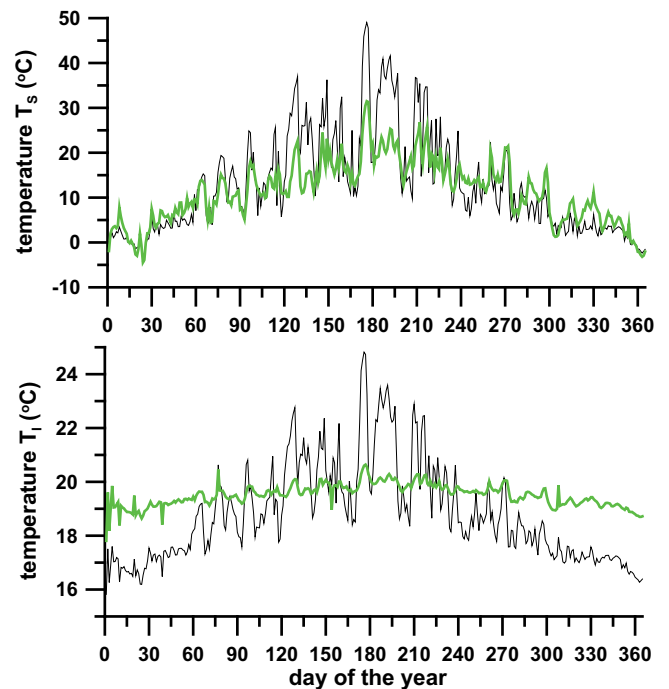


Figure 6: Annual variation of daily mean surface temperature T_s (above) and temperature at the under-site of the roof system T_I (below) for the concrete roof (black) and the green roof (green).

the temperature distribution in the atmosphere is quite similar to the one over the concrete slab. Inside the soil material a diurnal temperature variation is simulated following the cycle at the surface with a time lag. A further penetration is strongly decelerated and prevented by the insulation layer with a small thermal diffusivity.

The high surface temperature results in a very unstable thermal stratification of the near surface atmosphere. In nature, these conditions frequently cause thermal buoyant plumes to reduce or to balance the large temperature differences rapidly. However, in a one-dimensional model thermal plumes are excluded and an increased vertical diffusion, which is less efficient than small scale convection, should reduce the unstable stratification. Excluding thermal plumes by the model concept may result in an overestimation of the near surface temperatures especially during calm sunny summer days.

Diurnal variation of meteorological variables is modified significantly over the year due to changing synoptic conditions. Therefore, daily mean surface temperature shows large variations especially during summer, when clouds modify the strong radiative forcing. Due to the lower level of direct solar radiation in winter time, the day by day variation caused by clouds is much smaller. In Figure 6 the situation for a typical year in the first decade is presented. The surface of the concrete roof is heated up strongly especially in summer, while the green roof with a higher albedo and evapotranspiration shows much lower temperatures. It should be mentioned that the various model assumptions affect the temperature for the two roof situations considerably. For the

concrete roof a completely dry surface was assumed all the time, while in nature evaporation of standing water on sealed surfaces after precipitation events changes the heat energy budget and surface temperature significantly. During winter months, differences between surface temperatures of the two roof structures are much smaller with a tendency of a colder concrete roof. The mean surface temperature, calculated for the three summer months over the decade 2001–2010, shows a cooling effect of the green roof of 2.8 degrees compared to the concrete surface. In contrast, in winter the green roof is around 0.2 degrees warmer. The order of magnitude of the simulated results is very comparable to observations by TEEMUSK and MANDER (2009) or KÜNZEL (1999). The large temperature effects at the surface are smeared with increasing distance and at a height of 2 m above the roof the mean differences are smaller by around 1 degree for summer and almost negligible for winter season.

The heat flow through the concrete roofing system is large during summer and increases the inside mean temperature T_I (Figure 6). On the other hand, the green roof was found to be very effective in helping to keep the inside of a building cool. Temperature fluctuations over the year are small and the necessity of heating in winter and cooling in summer is reduced.

Although daily mean temperatures between the two roof systems mainly studied here do not differ greatly, temperature extremes on a sunny summer day can be significantly different for both situations (see Figure 4). In the field of biometeorology measures like hot days

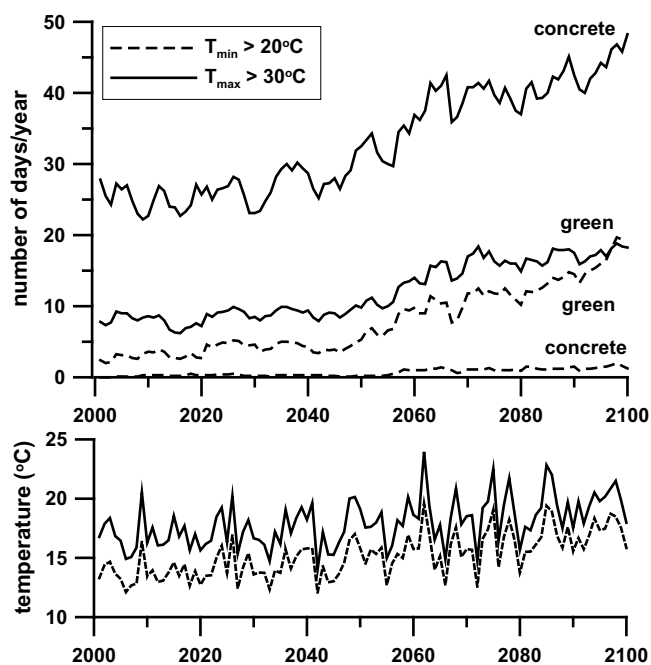


Figure 7: Simulated number per year of hot days and of tropical nights in this century above different roof structures (above) and simulated mean summer temperatures at 1 m height for a concrete roof (solid line) and a green roof (dashed line).

with a temperature maximum exceeding 30°C or tropical nights with minimum temperatures above 20°C are introduced in order to estimate thermal comfort conditions. One way to adapt cities to a future climate change is the inclusion of additional green spaces in urban environments in particular to reduce heat load related to high temperatures. As shown by LIU and BASKARAN (2003) the number of days with extreme temperatures over a concrete roof can be reduced significantly by a green roof.

Annual mean summer temperatures at 1 m height in the atmosphere are always 2–3 degrees higher for the concrete roof compared to the green roof (Figure 7). The simulated daily maximum and minimum temperatures have been evaluated with respect to the number of days per year exceeding the threshold values for hot days and for tropical nights given above. For a concrete roof a mean value of 25–28 hot days per year for the today situation has been simulated (Figure 7). This is a very common value for larger cities in Germany (FIEDLER, 1995). For a green roof a significantly lower value of 8–10 days is simulated. The expected regional temperature rise in the next 100 years of 3–4 K will increase the probability of the occurrence of temperature extremes as well. Since the regional climate change is included in the CLM forcing, an increased risk of maximum temperatures above 30°C is simulated with an expected number of 40–50 days per year at the end of this century. For the green roof situation the number of hot days will only reach values of 15–18 days for the same time period.

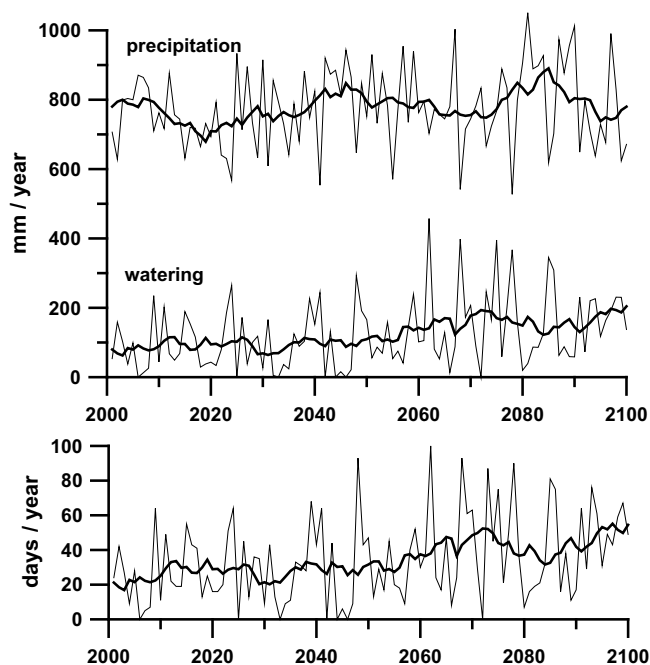


Figure 8: Annual precipitation (from the regional climate model) and estimated additional watering (above) and watering days (below). Thick curves are 10 year running means.

On the other hand, the reduced surface cooling during night time for the vegetated roof results in higher temperatures and a larger number of situations with a tropical night ($T_{min} > 20^{\circ}\text{C}$). Currently, the average frequency per year for the concrete roof is well below one and for the green roof 3–4 nights per year are simulated. A regional climate warming will increase the number to 2–3 nights for the concrete roof structure and to a significant number, around 15 nights, for the green roof situation. Based on these results one can conclude that in summer a green roof will reduce the local heat load above the surface for the day time situation but will increase the local discomfort during night.

It should be mentioned here again that these findings should be interpreted as a rough orientation because of all the assumptions made in this study. One main assumption was the existence of an always green surface on the green roof for the whole simulation period. Given the expected seasonal shift in precipitation, with an increase in winter and a decrease during the summer months, a risk of droughts is likely. In order to ensure the functionality of the green roof with respect to temperature, additional watering will become more regular in the future.

The water balance of the green roof can be estimated by the knowledge of time series of precipitation, water loss by evapotranspiration and water storage in the soil material. If water balance is negative, the deficit will be substituted by additional watering. Assuming a field capacity of 40 mm for the 10 cm substrate layer of the green roof (LIESECKE, 2005) and a complete availabil-

ity of the soil water for the vegetation the amount of additional water and the number of watering days per year can be estimated.

Regional climate model results show almost no trend for annual precipitation (Figure 8) but a seasonal shift from summer to winter. However, the year to year variation is large resulting in a rain water quantity ranging from 500 mm to more than 1000 mm. Due to an increased temperature in the next 100 years and a decreasing cloud coverage in summer, as predicted by the regional climate model, evapotranspiration can be expected to be large. Together with a reduction in summer precipitation the need for watering is estimated to increase from 100 mm per year today up to 200 mm at the end of this century, however, with a large year to year variation. The number of watering days increases in the same period from 20 to 50–60 days.

4 Conclusions

In this paper a numerical simplified surface layer model was adopted to simulate temperature in and above extensive roofs of different structures. Forced by the results of a regional climate model, temperature variation for very different time scales from days to decades have been calculated.

The applicability of the model has been tested by a comparison with the results of a selected field experiment. Surface temperatures for different substrate layers have been reasonably reproduced by the model as well as temperatures inside the roof structures. The results of the long term simulation also show a wide range of typical differences between the temperature distributions for a green roof compared to a concrete one, which are well known from field experiments.

The diurnal variation of temperature for different roof structures demonstrates the effectiveness of green roofs in protecting living space beneath the roof against ambient temperature extremes. In the summer period the green roof significantly decreases temperature fluctuations compared to a bare concrete roof. For the situation presented in this paper, typical mean summer surface temperature was lowered approximately by 2.8 degrees, while in winter time, the green roof is approximately 0.2 degrees warmer. However, these values are valid only for the specific thermal properties used in this study and for the specific year presented above. For all other summer and winter months of the 100 year simulation period the order of magnitude and sign is very similar but with year-to-year variation.

The characteristic effects of a green roof in lowering temperature extremes also have consequences for the human comfort in cities. Green spaces can significantly reduce the number of hot days per year and therefore have a great potential in adapting cities for global warming. On the other hand, the green roof is warmer during nights and in summer this results in higher night time

temperatures and possibly in an increase of human discomfort.

The potential of a green roof for lowering the temperature extremes is only given for a living vegetation cover. Since a seasonal shift in precipitation with an increase in winter and a decrease in the summer months is likely, a larger risk of droughts is given in the future. In order to ensure the functionality of the green roof with respect to temperature, additional watering will be more regular. An estimation of the future water requirement is given.

The soil water content was not simulated in this study. However, this should be an important improvement of the model in the near future in order to estimate the effects on evapotranspiration during drying periods or for times after precipitation events.

Acknowledgments

The author would like to thank the reviewers for their careful reading and very useful comments, which improved the quality of the paper significantly. This research was supported by the Federal Ministry of Education and Research (Bundesministerium für Bildung und Forschung BMBF) under 01 LS 05038A. The author would like to thank also the Model and Data Group (M&D) at the German Climate Computing Centre (DKRZ), Hamburg, for providing the CLM model data.

References

- ALEXANDRI, E., P. JONES, 2007: Developing a one-dimensional heat and mass transfer algorithm for describing the effect of green roofs on the building environment: Comparison with experimental results. – *Build. Environ.* **42**, 2835–2849.
- ALEXANDRI, E., P. JONES, 2008: Temperature decrease in an urban canyon due to green walls and green roof in diverse climates. – *Build. Environ.* **43**, 480–493.
- BUSINGER, J.A., J.C. WYNGAARD, Y. IZUMI, E.F. BRADLEY, 1971: Flux-profile relationships in the atmospheric surface layer. – *J. Atmos. Sci.* **28**, 181–189.
- DYER, A.J., 1974: A review of flux-profile relationships. – *Bound.-Layer Meteor.* **7**, 363–372.
- FIEDLER, F., 1995: *Klimaatlas Oberrhein Mitte-Süd*. – Vdf Hochschulverlag, ETH Zürich.
- GAFFIN, S.R., R. KHANBILVARDI, C. ROSENZWEIG, 2009: Development of a green roof environmental monitoring and meteorological network in New York city. – *Sensors* **9**, 2647–2660.
- GILL, S.E., J.F. HANDLEY, A.R. ENNOS, S. PAULEIT, 2007: Adapting cities for climate change: The role of green infrastructure. – *Built Environ.* **33**, 115–133.
- GROSS, G., 1993: *Numerical simulation of canopy flows*. – Springer Verlag Heidelberg, 167 pp.
- HARAZONO, Y., S. TERAOKA, I. NAKASE, H. IKEDA, 1990: Effects of rooftop vegetation using artificial substrates on the urban climate and thermal load of buildings. – *Energy Build.* **15**, 435–442.

- HOLLWEG, H.-D., U. BÖHM, I. FAST, B. HENNEMUTH, K. KEULER, E. KEUP-THIEL, M. LAUTENSCHLAGER, S. LEGUTKE, K. RADTKE, B. ROCKEL, M. SCHUBERT, A. WILL, M. WOLDT, C. WUNRAM, 2008: Ensemble simulations over Europe with the regional climate model CLM forced with IPCC ARA4 global scenarios. – CLM Technical Report No. 3, Max Planck Institute for Meteorology, Hamburg.
- HUPFER, P., W. KUTTLER, 2006: Witterung und Klima. – Teubner Verlag, 554 pp.
- HUTTNER, S., M. BRUSE, P. DOSTAL, 2008: Using ENVI-met to simulate the impact of climate warming on the microclimate in central European cities. – Berichte Meteor. Inst. Univ. Freiburg **18**, 307–312.
- IPCC, 2007. Cambridge University Press, Cambridge UK.
- JENDRITZKY, G., G. HAVENITH, P. WEIHS, E. BATCHVAROVA (Eds), 2009: Towards a universal thermal climate index UTCI for assessing the thermal environment of human beings. – Final report Cost action 730.
- KÖHLER M., W. MALORNY, 2009: Wärmeschutz durch extensive Gründächer. Europäischer Sanierungskalender 2009. H. VENSNER, H. (Ed.). – Beuth Verlag.
- KÜNZEL, H.M., 1999: Einfluß der Deckschicht auf die Temperaturverhältnisse in Flachdächern. Mitteilung des Fraunhofer-Instituts für Bauphysik 26 (1999).
- KUTTLER, W., 2011: Climate change in urban areas, Part 1, Effects. – Environmental Science Europe (ESEU), Springer open, DOI:10.1186/2190-4715-23-11, 1–12.
- LAUTENSCHLAGER, M., K. KEULER, C. WUNRAM, E. KEUP-THIEL, M. SCHUBERT, A. WILL, B. ROCKEL, U. BOEHM, 2009: Climate simulation with CLM, Scenario A1B run no.1, Data Stream 3: European region MPI-M/MaD. – World Data Center for Climate. DOI:DOI:10.1594/WDCC/CLM_A1B_1.D3.
- LIESECKE, H.-J., 2005: Jährliche Wasserrückhaltung durch extensive Dachbegrünungen. – Dach+Grün **14**, 4–13.
- LIU, K.K.Y., B.A. BASKARAN, 2003: Thermal performance of green roofs through field evaluation. – Proceedings for the First North American Green Roof Infrastructure Conference, Awards and Trade Show (Chicago, IL, 5/29/2003), 1–10, May 29, (NRCC-46412).
- LIU, K.K.Y., J. MINOR, 2005: Performance evaluation of an extensive green roof. Greening Rooftops for Sustainable Communities (Washington, D.C. 5/5/2005), pp. 1-11, May 01, (NRCC-48204)
- MUTHERS, S., A. MATZARAKIS, E. KOCH, 2010: Climate change and mortality in Vienna – A human biometeorological analysis based on regional climate modelling. – Int. J. Environ. Res. Public Health **7**, 2965–2977.
- ROCKEL B., A. WILL, A. HENSE, 2008: Regional climate modelling with COSMO-CLM. – Meteorol. Z. **17**, 347–528.
- STULL, R.B., 1988: An introduction to boundary layer meteorology. – Kluwer Academic, 666 pp.
- TAKEBAYASHI, H., M. MORIYAMA, 2007: Surface heat budget on green roof and high reflection roof for mitigation of urban heat island. – Build. Environ. **42**, 2971–2979.
- TAKAKURA, T., S. KITADE, E. GOTO, 2000: Cooling effect of greenery cover over a building. – Energy Build. **31**, 1–6.
- TEEMUSK, A., Ü. MANDER, 2009: Greenroof potential to reduce temperature fluctuations of a roof membrane: A case study from Estonia. – Build. Environ. **44**, 643–650.
- WALTER, A., K. KEULER, D. JACOB, R. KNOCH, A. BLOCK, S. KOTLARSKI, G. MÜLLER-WESTERMEIER, D. RECHID, W. AHRENS, 2006: A high resolution reference data set of German wind velocity 1951–2001 and comparison with regional climate model results. – Meteorol. Z. **15**, 585–596.
- WILBY, R.L., 2007: A Review of Climate Change Impacts on the Built Environment. – Built Environ. **33**, 31–45.